THE JOURNAL OF BIOLOGICAL CHEMISTRY
Vol. 275, No. 19, Issue of May 12, pp. 14321–14330, 2000
Printed in U.S.A.
© 2000 by The American Society for Biochemistry and Molecular Biology, Inc.

Identification of the Residues in the Extracellular Region of KDR Important for Interaction with Vascular Endothelial Growth Factor and Neutralizing Anti-KDR Antibodies*

Received for publication, November 1, 1999, and in revised form, February 11, 2000

Dan Lu‡, Paul Kussie§, Bronislaw Pytowski‡, Kris Persaud‡, Peter Bohlen¶, Larry Witte‡, and Zhenping Zhu‡‖

From the Departments of ‡Molecular and Cell Biology, §Protein Chemistry, and ¶Research, ImClone Systems Incorporated, New York, New York 10014

The kinase domain receptor (KDR) of vascular endothelial growth factor (VEGF) is the main human receptor responsible for the angiogenic activity of VEGF. The extracellular region of KDR is comprised of seven immunoglobulin-like domains, of which the first three have been shown to be required for ligand binding. We have previously described antibodies directed against the extracellular region of KDR, including MAB383 and MAB664, which were shown to block the binding of VEGF to the receptor and to inhibit both VEGF-induced mitogenesis of human endothelial cells *in vitro* and tumor growth *in vivo*. Here we generated a series of KDR deletion mutants consisting of truncated extracellular regions and mapped out the domain(s) responsible for binding to VEGF and the neutralizing anti-KDR antibodies. All neutralizing antibodies were found to require domain 3 for efficient binding. Alanine-scanning mutagenesis of domain 3 identified two different sets of five residues, Ile^{256}, Asp^{257}, Glu^{261}, Leu^{313}, and Thr^{315} and Tyr^{262}, Pro^{263}, Ser^{264}, Ser^{265}, and Lys^{266}, that were critical for binding to MAB383 and MAB664, respectively. Combination of alanine mutations affecting both MAB383 and MAB664 binding resulted in a variant that also lost binding to VEGF. These results suggest that the residues within this region of domain 3 are critical for VEGF binding. Our studies provide a basis for the mechanism of action of our anti-KDR antibodies and establish a functional foundation for the development of other classes of antagonists to the receptor.

KDR, the kinase domain receptor of VEGF[1] (also known as VEGF receptor 2), is the main human receptor responsible for the angiogenic activity of VEGF (1–3). There is compelling evidence to suggest that VEGF/KDRs play an important role in tumor angiogenesis, a process essential for both tumor growth and metastasis (for reviews see Refs. 4–6). Inhibition of tumor growth and metastasis in a variety of animal models has been achieved by various approaches that disrupt and/or neutralize the functions of either VEGF or KDR (6–9). Further, VEGF/KDR pathway has also been implicated in several other pathological processes, including diabetic retinopathy and rheumatoid arthritis (10, 11). Antagonists to VEGF and/or KDR, therefore, may have broad applications in the treatment of a variety of human diseases where pathological angiogenesis is involved.

VEGF is a member of the cysteine-knot growth factor family that also includes several other factors, such as platelet-derived growth factor, transforming growth factor β, and nerve growth factor (12). VEGF exists as a homodimer held together by two intermolecular disulfide bonds. A high resolution crystal structure of VEGF has been recently determined (13, 14). Each VEGF homodimer possesses two symmetrical binding surfaces, one located at each pole of the molecules, and is composed of binding determinants contributed by both subunits in the homodimer. Within each binding surface eight residues form two "hot spots"; the larger one consists of Ile^{43}, Ile^{46}, Ile^{83}, Lys^{84}, and Pro^{85} from one subunit, along with one residue, Glu^{64}, from the other subunit, and the smaller one contains one residue from each subunit, Gln^{79} and Phe^{17} (13–15). Recent studies have demonstrated that a single VEGF homodimer binds two molecules of KDR, which is followed by receptor dimerization and activation (13, 14, 16). The extracellular region of KDR consists of seven immunoglobulin-like domains, and deletion studies have shown that domains 1–3 are sufficient and necessary for high affinity binding to VEGF (16, 17). Deletion of domain 3 alone reduced the binding to VEGF by >1000-fold, indicating a critical functional role for this domain in VEGF/KDR interaction (16, 17). Because no detailed structural information on KDR is available to date, the molecular basis of VEGF/KDR interaction is poorly understood.

We previously described a panel of antibodies that recognize various epitopes on the extracellular region of KDR (18). All eight neutralizing antibodies that block VEGF/KDR interaction, including MAB383, MAB664, and IMC-1C11, were found to require domain 3 for efficient binding, whereas all nonblocking antibodies recognize epitopes that are located outside this domain.[2] It is noteworthy that none of our neutralizing anti-KDR antibodies cross-reacts with fetal liver kinase 1 (Flk-1), the mouse homolog of KDR, despite high sequence identity (~85%) between the two molecules. Both KDR and Flk-1, however, bind and can be activated by human VEGF. Taken together, these observations suggest that our neutralizing anti-KDR antibodies interact with distinct epitopes on KDR molecule. Using alanine-scanning mutagenesis, we have characterized the functional epitopes within KDR domain 3 for binding to neutralizing anti-KDR antibodies and to the natural

* The costs of publication of this article were defrayed in part by the payment of page charges. This article must therefore be hereby marked "*advertisement*" in accordance with 18 U.S.C. Section 1734 solely to indicate this fact.

‖ To whom correspondence should be addressed: Dept. of Molecular and Cell Biology, ImClone Systems Incorporated, 180 Varick St., New York, NY 10014. Tel.: 212-645-1405; Fax: 212-645-2054; E-mail: zhenping@imclone.com.

[1] The abbreviations used are: VEGF, vascular endothelial growth factor; Flk-1, fetal liver kinase 1; Flt-1, Fms-like tyrosine kinase-1; scFv, single chain Fv; AP, alkaline phosphatase; PCR, polymerase chain reaction; HRP, horseradish peroxidase; PBS, phosphate-buffered saline; ELISA, enzyme-linked immunosorbent assay.

[2] Z. Zhu, unpublished observations.

This is an Open Access article under the CC BY license.

Exhibit 2082
Page 01 of 10

Samsung v. Regeneron
IPR2023-00442
U.S. Pat. 10,130,681, Exhibit 2082

ligand, VEGF. Our studies indicate that two neutralizing anti-KDR antibodies, MAB383 and MAB664, bind to nonoverlapping epitopes within domain 3. Further, we have identified a subset of residues within this domain important for binding to VEGF. Taken together, our data provide a basis for the mechanism of action of our anti-KDR antibodies and for developing other classes of antagonists to the receptor.

EXPERIMENTAL PROCEDURES

Generation of Anti-KDR Antibodies—A panel of anti-KDR antibodies were generated from mice immunized with a fusion protein consisting of the full extracellular region of KDR fused to human alkaline phosphatase (AP), using both conventional hybridoma technique and antibody phage display library as described previously (19). Briefly, MAB383, MAB664, and MAB413 are hybridoma-derived murine monoclonal antibodies (18); IMC-1C11 is a mouse/human chimeric IgG1 antibody constructed from a single chain Fv (scFv) isolated from a phage display library (19, 20); and DAB p3S5 is a diabody (a bivalent scFv dimer) constructed from a scFv isolated from the same phage display library (21).

Generation of KDR Deletion Mutants—Soluble mutant proteins consisting of various lengths of the extracellular region of KDR fused to AP were expressed in mammalian cells. The definition of KDR deletion mutants are as follows (see also Fig. 1*A*): KDR (1–7), the full-length KDR extracellular region containing all the seven domains of the receptor (from Met^1 to Val^{742}); KDR (1–5), the mutant containing the five N-terminal domains (from Met^1 to Glu^{552}); KDR (1–4), the mutant containing the four N-terminal domains (from Met^1 to Pro^{403}); KDR (1–3), the mutant containing the three N-terminal domains (from Met^1 to Lys^{327}); KDR (1–2), the mutant containing the two N-terminal domains (from Met^1 to Tyr^{224}); KDR (1), the mutant containing the first N-terminal domain only (from Met^1 to Asp^{131}); KDR (2–7), the mutant containing KDR domains 2–7 (from Pro^{124} to Val^{742}); and KDR (3–7), the mutant containing KDR domains 3–7 (from Asp^{225} to Val^{742}). All KDR deletion mutants were generated by PCR using a template comprising the chimeric cDNA encoding sequences for the full-length KDR extracellular region fused to AP (19, 22). The PCR fragments were digested with restriction enzymes *Rsr*II and *BspE*I and cloned into expression vector KB98.2, a derivative of AP tag (22). In this vector, the KDR deletion mutants were expressed as soluble AP fusion proteins. Each of the DNA constructs was used to transfect NIH 3T3 cells for transient expression, and the fusion proteins were purified from the condition medium using anti-AP antibody affinity chromatography as described previously (19).

Binding of the KDR Deletion Mutants to VEGF and Anti-KDR Antibodies—The KDR deletion mutants were first immobilized onto 96-well plates (Nunc, Rosklide, Denmark) using a rabbit anti-AP antibody (DAKO Immunoglobulins, Glostrup, Denmark) as the capturing agent. The plates were then incubated with various anti-KDR antibodies at room temperature for 1 h, followed by incubation with goat anti-mouse-HRP conjugate for MAB383, MAB664, MAB413, and DAB p3S5 or goat anti-human κ chain antibody-HRP conjugate for IMC-1C11 (19, 20). The plates were washed and developed as described previously (19, 21). For VEGF binding, the KDR deletion mutants were incubated with VEGF coated plates, followed by detection with a rabbit anti-AP antibody-HRP conjugate (21).

Phagemid Construction for Phage Displaying of KDR Domain 3—A gene segment encoding KDR domain 3 (from Tyr^{221} to Ser^{334}) was amplified by PCR using the following primers:

5′-CTG ATA GCG GCC CAG CTG GCC ATG GCC TAT AGG ATT TAT GAT-3′
Sfi I site

5′-AGT TTC TGC GGC CGC ATG GCG TCC TTC TAT ACT TCC AAA AGC AAC-3′
Not I site Factor Xa site

SEQUENCES 1 AND 2

The DNA fragment (~400 base pairs) was purified on agarose gel, digested with *Sfi*I and *Not*I, and ligated into the pCANTAB 5E phagemid vector (Amersham Pharmacia Biotech) to create the construct phKDR-D3. In this construct KDR domain 3 is inserted between the leader sequence and the encoding sequence of the M13 gene III for displaying on phage surface (see Fig. 3, *top panel*). For assay purposes, a short DNA segment encoding a factor Xa cleavage site and a 13-amino acid-long polypeptide tag, the E tag (19), were inserted between the C terminus of KDR and the gene III sequence.

Alanine Mutagenesis and Phage Preparation—Mutations in phKDR-D3 were made by PCR-based site-directed mutagenesis using the QuickChange™ kit (Strategene, La Jolla, CA), following the manufacturer's instructions and were confirmed by DNA sequencing. *Escherichia coli* strain TG1 cells were transformed with the phagemid and selected on 2× YTAG plates (2× YT plus ampicillin at 100 μg/ml and 2% glucose) as described previously (19). To prepare monovalent phage, individual TG1 colonies were grown at 37 °C in 2× YTAG medium to log phase, infected with M13 KO7 helper phage (Strategen), and grown overnight at 30 °C in 2× YTAK medium (2× YTA plus kanamycin at 50 μg/ml) to produce phage particles. The *E. coli* cells were removed by centrifugation, and the culture supernatant was mixed with ⅕ volume of 25% PEG (molecular weight, 8000)/2.5 M NaCl and centrifuged at 20,000 × *g* for 20 min to precipitate the phage particles. The phage pellet was resuspended in PBS, and the phage titer was determined (23).

Binding of the Phage-displayed KDR Domain 3 Mutants to Anti-KDR Antibodies—96-well Maxi-sorp plates (Nunc) were coated with either anti-E tag antibody (Amersham Pharmacia Biotech) or various anti-KDR antibodies (100 μl/well at 1 μg/ml in PBS) overnight at 4 °C. The plates were washed twice with PBS and incubated with blocking buffer (3% fat-free milk in PBS) at 37 °C for 2 h. The amplified phage were blocked with ⅙ volume of 18% milk/6× PBS at room temperature for 2 h and serially diluted in blocking buffer and then transferred to the antibody-coated plates. After 1 h of incubation at room temperature, the plates were washed three times with PBS/0.2% Tween-20, followed by incubation with an anti-M13 antibody-HRP conjugate (Amersham Pharmacia Biotech, 1:5000 dilution) in blocking buffer for an additional 1 h. The plates were washed four times with PBS/0.2% Tween-20, developed using the TMB peroxidase substrate (KPL, Gaithersburg, MD), stopped with 1 M H_2SO_4, and read spectrophotometrically at 450 nm (19). Binding of each alanine mutant to anti-KDR antibodies was calculated as a relative value to that of the wild type domain 3 following the formula: Relative binding of alanine mutant = R(mut)/R(wt), where

$$R(\text{mut}) = \frac{\text{Mutant binding } (A_{450\,\text{nm}}) \text{ to anti-KDR antibody}}{\text{Mutant binding } (A_{450\,\text{nm}}) \text{ to anti-E tag antibody}} \quad \text{(Eq. 1)}$$

$$R(\text{wt}) = \frac{\text{Wild-type binding } (A_{450\,\text{nm}}) \text{ to anti-KDR antibody}}{\text{Wild-type binding } (A_{450\,\text{nm}}) \text{ to anti-E tag antibody}} \quad \text{(Eq. 2)}$$

Expression of KDR (1–3) Variants in Mammalian Cells—Mutations within domain 3 were generated by overlapping PCR using KDR (1–3)-AP fusion protein (Fig. 1*A*) as the template and confirmed by DNA sequencing. The plasmids were used to transfect COS-7 cells for transient expression followed the procedure previously described (20). The conditioned media were collected at 48 and 96 h after transfection, pooled, and concentrated using Centricon-10 (Amicon Corp., Beverly, MA). The concentration of each protein variant was determined by Western blot analysis using an anti-AP antibody as the detecting agent.

Binding of KDR (1–3) Variants to Anti-KDR Antibodies and VEGF—96-well Maxi-sorp plates were coated with VEGF165 or various anti-KDR antibodies (100 μl/well at 1 μg/ml in PBS) overnight at 4 °C. The plates were washed twice with PBS and incubated with blocking buffer at 37 °C for 2 h, followed by incubation with KDR (1–3)-AP variants at room temperature for additional 1 h. The plates were washed four times with PBS/0.2% Tween-20, followed by incubation with p-nitrophenyl phosphate (Sigma), a substrate of AP, to quantitate the bound AP activity (19). DAB p3S5, an anti-KDR diabody that binds to KDR domain 1, was used in this assay in parallel to other anti-KDR antibodies and VEGF, to ensure the functional expression of the variant protein and to normalize the amount of protein added in each assay. Binding of each KDR (1–3) variant to anti-KDR antibodies and VEGF was calculated as a value relative to that of the wild type KDR (1–3) following the formula described above for the phage ELISA. The binding of KDR (1–3) variants to diabody DAB p3S5 was used as the reference instead of that to anti-E tag antibody.

Homology Modeling of KDR Domain 3—A model of KDR domain 3 of was constructed using the crystal structure of telokin, an abundant smooth muscle protein with an amino acid sequence identical to that of the C-terminal region of smooth muscle myosin light chain kinase (Protein Data Bank identification number 1TLK) (24) as a template. The crystal structure of Fms-like tyrosine kinase-1 (Flt-1) domain 2 (Protein Data Bank identification number 1FLT) (25) was used as a reference for model building. The sequences of telokin and KDR domain 3 were aligned based on conserved amino acids according to the guidelines described by Harpaz and Chothia (27) for immunoglobulin domains. The three-dimensional model was built using the program O (26). The KDR domain 3 side chains were substituted on the telokin

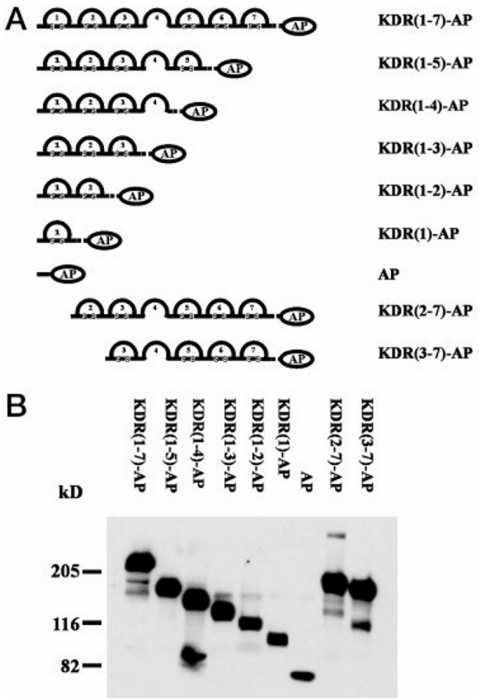

FIG. 1. **Expression of KDR deletion mutants in NIH 3T3 cells.** *A*, a schematic diagrams showing the seven KDR extracellular domains, KDR(1–3)-AP, and various KDR deletion mutants consisting of different lengths of the extracellular region. The domains are numbered from the N terminus. *B*, SDS-polyacrylamide gel electrophoresis analysis of the affinity purified KDR deletion mutant-AP fusion proteins.

template maintaining similar orientation. In the two sites where KDR domain 3 had an insertion relative to telokin, a two-residue loop extension was built manually, and a seven-residue strand-loop-strand segment was modeled using the O search algorithm of Protein Data Bank-derived structures.

RESULTS

Expression of KDR Deletion Mutants—To determine the minimal domain requirements for VEGF binding and to map out the binding domains for various antibodies, a series of KDR deletion mutants were produced. Each of the seven domains of KDR was deleted from the C terminus of the extracellular region (Fig. 1*A*). Additional two mutants were made by removing the first or the first plus the second domains from the N terminus of the extracellular region (Fig. 1*A*). The mutants were expressed in NIH 3T3 cell lines as fusion proteins to AP and purified by affinity chromatography. SDS-polyacrylamide gel electrophoresis analysis of purified proteins demonstrated that all KDR mutants gave rise to a major band with mobility close to that anticipated (Fig. 1*B*).

Binding of VEGF and Anti-KDR Antibodies to KDR Deletion Mutants—Systematic C-terminal domain deletion of KDR showed no effect on its binding to VEGF until domain 3 was deleted; deletion of domain 3 completely abolished the binding of VEGF (Fig. 2). Deletion the first domain from the N-terminal of KDR reduced its binding to VEGF by ~85%, and no binding was seen when both the first and the second N-terminal domains were deleted. These data suggest that all the three N-terminal domains of KDR are important and sufficient for high affinity binding to VEGF.

The binding domain(s) of various anti-KDR antibodies were also mapped using the deletion mutants (Fig. 2). MAB383 and MAB664 both bound to all mutants containing domain 3, thus locating their binding epitope(s) within this domain. MAB413 bound to full-length KDR, KDR (2–7), and KDR (3–7) but not to other mutants, *e.g.* KDR (1–5), indicating that it binds epitope(s) within domain 6 and 7. In contrast, DAB p3S5 bound to all mutants except KDR (2–7) and KDR (3–7), locating its binding epitope to domain 1. IMC-1C11 bound to KDR deletion mutants in a pattern very similar to VEGF, both of which require domains 1–3 (Fig. 2).

We have shown that MAB383, MAB664, and IMC-1C11, but not MAB413 and DAB p3S5, were capable of competing with VEGF for binding to KDR (Ref. 18 and Table I). Together with the domain mapping data, this suggests KDR domain 3 plays a critical role in VEGF binding.

KDR Domain 3 Expression on Filamentous Phage Surface—To dissect out the amino acid residues in domain 3 critical for binding to VEGF and our anti-KDR antibodies, we cloned the gene segment encoding the domain into a phagemid vector for displaying on phage surface (Fig. 3, *top panel*). A short piece of DNA encoding a factor Xa cleavage site, as well as a polypeptide tag, the E tag, were inserted between the C-terminal of KDR coding sequence and the gene III coding sequence for assay purposes (Fig. 3, *top panel*). The phage surface-displayed KDR domain 3 bound efficiently to MAB383 and MAB664 but not to IMC-1C11 and VEGF (Fig. 3, *middle panel*). This is consistent with our earlier observation that both IMC-1C11 and VEGF require all three N-terminal domains for high affinity binding (Fig. 2). Incubation with a reducing agent, dithiothreitol, to break the disulfide bond within the domain, reduced the binding of the KDR phage to MAB383 and MAB664 by ~60–70%. The binding to both MAB383 and MAB664 was completely abolished when the KDR phage was treated with factor Xa prior to the assay (Fig. 3, *middle panel*). The binding to an anti-E tag antibody, however, was not affected by treatment with either dithiothreitol or Factor Xa. Taken together, these observations indicate that KDR domain 3 is properly folded and functionally displayed on the phage surface.

Fig. 3 (*bottom panel*) shows the dose-dependent binding of KDR phage to both anti-KDR monoclonal antibodies and anti-E tag antibody. Within the range of phage titers from 5×10^8 to 1.6×10^{10} plaque-forming units/ml, a good linear relationship was seen between the numbers of phage added and the absorbance at 450 nm ($A_{450\ \mathrm{nm}}$) in all three binding assays. Based on this observation, phage titers between 1 and 10×10^9 plaque-forming units/ml were used in our subsequent ELISA assays for all alanine mutants.

Construction of Alanine Mutants of KDR Domain 3—Despite overall high sequence identity (~85%) between KDR and its murine homolog, Flk-1, none of the neutralizing anti-KDR antibodies produced in our laboratory cross-react with Flk-1 (18, 19). A sequence alignment between KDR and Flk-1 revealed that the most divergent region among the seven domains is domain 3 with only ~74% identity (Fig. 4*A*). MAB383 and MAB664 did not bind to either full-length Flk-1 or Flk-1 domain 3 displayed on phage surface (not shown). On the other hand, both KDR and Flk-1 bind and can be activated by human VEGF. These observations suggest that our neutralizing anti-KDR antibodies interact with distinct epitopes in KDR molecule that are not present in Flk-1. By aligning the amino acid sequences of KDR and Flk-1, twenty-eight residues that differ within domain 3 were selected for mutagenesis. The 28 residues were grouped in clusters so that, in total, six mutants were constructed (M1–M6), with each mutant containing four to eight alanine mutations (Fig. 4*A*).

Molecular Modeling of KDR Domain 3—Immunoglobulin domains are formed by two β-sheets packed together, with variations in β-strand length and in the conformation of the loops connecting the strands. By examining proteins within the immunoglobulin superfamily, Harpaz and Chothia (27) has clas-

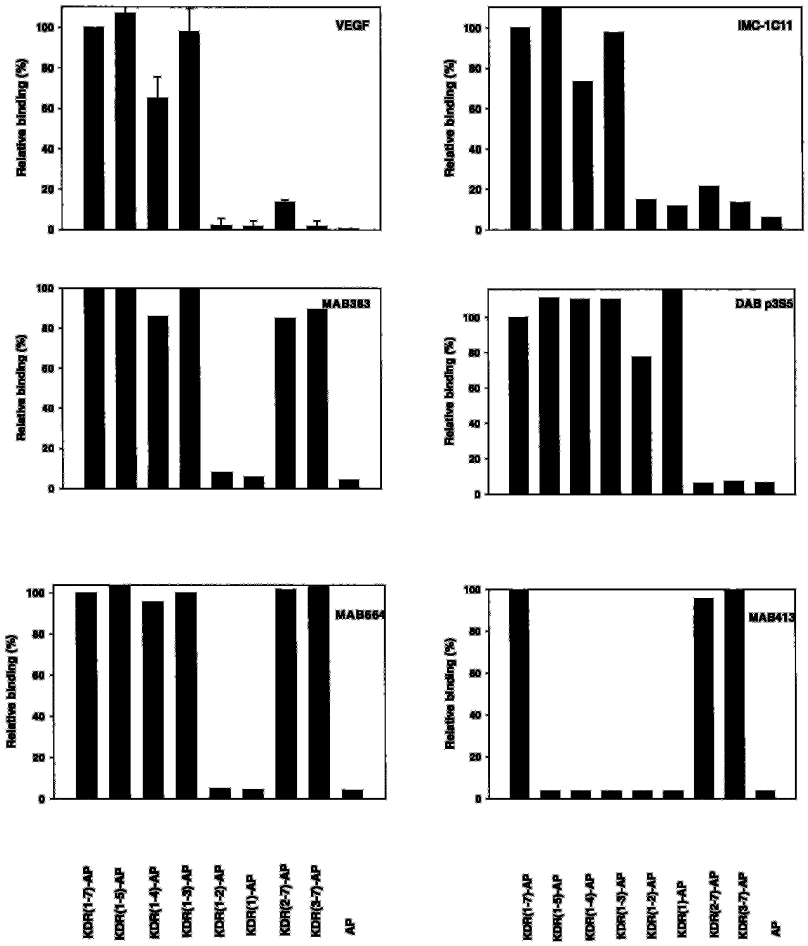

FIG. 2. **Binding of KDR deletion mutants to VEGF and anti-KDR antibodies.** The KDR deletion mutants were captured onto 96-well plates with a rabbit anti-AP antibody, followed by incubation with various anti-KDR antibodies. The plates were detected using goat anti-mouse-HRP conjugate for MAB383, MAB664, MAB413, and DAB p3S5 or goat anti-human κ chain antibody-HRP conjugate for IMC-1C11. For VEGF binding, the KDR deletion mutants were incubated with VEGF-coated plates, followed by detection with a rabbit anti-AP antibody-HRP conjugate.

TABLE I
Characteristics of anti-KDR antibodies

Antibody or VEGF	Properties	Binding epitope(s) on KDR	KDR/VEGF blocking[a]	Cross-competition for binding KDR[b]				
				MAB383	MAB664	MAB413	IMC-1C11	DAB p3S5
MAB383	Murine, IgG1	Domain 3	Yes	+	−	−	+	−
MAB664	Murine, IgG1	Domain 3	Yes	−	+	−	−	−
MAB413	Murine, IgG1	Domains 6 and 7	No	−	−	+	−	−
IMC-1C11	Chimeric, IgG1	Domains 1–3	Yes	+	−	−	+	−
DAB p3S5	Murine, diabody	Domain 1	No	−	−	−	−	+
VEGF	Human VEGF165	Domains 1–3	Yes	+	+	−	+	−

[a] Determined by an *in vitro* ELISA as previously described (18). Briefly, the antibodies were first mixed with a fixed amount of KDR(1–7)-AP fusion protein (50 ng) and incubated at room temperature for 1 h. The mixtures were then transferred to a 96-well plate precoated with VEGF165 (200 ng/well) and incubated at room temperature for 2 h. The plate was washed, and an AP substrate (*p*-nitrophenylphosphate; Sigma) was added to quantify the bound KDR(1–7)-AP molecules. The effect of anti-KDR antibodies on blocking the binding of KDR to immobilized VEGF was determined.

[b] Determined by BIAcore analysis using KDR(1–7)-AP-coated biosensor chips (18). Briefly, KDR-AP fusion protein was immobilized onto a biosensor chip, and antibodies or VEGF were injected sequentially, in pairs, to determine the effect of the first antibody binding to KDR upon the binding of the second antibody (or VEGF). + indicates that two antibodies, or antibody and VEGF, cross-compete with each other for binding to KDR, whereas − indicates the antibodies (or VEGF) do not compete with each other for KDR binding.

sified immunoglobulin domains into four structural sets, the V, C1, C2, and I sets, based on similarities in sequence and structure. KDR domain 3 is a member of the I structural set within the immunoglobulin superfamily. It matches exactly the profile of the 20 key amino acids that define the I set, consisting of packing residues at the core of the domain. KDR domain 3 was modeled using the crystal structure of the I set member, telokin, as the template, by inserting two residues in the loop connecting strands B and C and seven residues between strands D and E to increase the length of these strands (Fig. 4*B*). After examination of the model, the residues selected for mutagenesis were found to be clustered generally along β-strands A (M1), C and C′ (M2 and M6), D and E (M3), and G (M5). Cluster 4 (M4) was located in the loop connecting β-strands E and F.

Binding of KDR Domain 3 Alanine Mutants to MAB383 and MAB664—A phage ELISA was used to test binding of the phage-displayed domain 3 alanine mutants to immobilized antibodies. As a control for surface displaying and for quantitation of numbers of phages added in the ELISA assay, all the mutants were also tested in parallel for binding to an anti-E tag antibody.

We have previously shown that MAB383 and MAB664 bind to nonoverlapping epitope(s) (18), and our results with alanine-

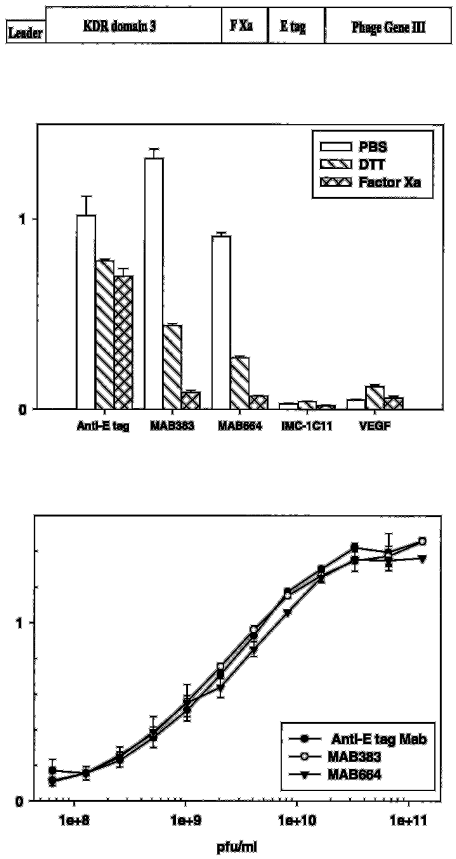

FIG. 3. **Binding of phage surface-displayed KDR domain 3 to anti-KDR antibodies.** *Top panel*, a schematic diagram showing the DNA construct for displaying KDR domain 3 on M13 bacteriophage surface. The KDR domain 3 was inserted between the leader and the encoding sequences of gene III coat protein of the phage. Note that a factor Xa cleavage site and a peptide tag, the E tag, were inserted between the encoding sequences of KDR domain 3 and the gene III protein. *Middle panel*, binding of the phage surface-displayed KDR domain 3 to anti-KDR antibodies and VEGF under various conditions. Binding of the KDR phage to anti-E tag antibody was used as the positive control to ensure the surface displaying of the polypeptide. *Bottom panel*, dose-dependent binding of KDR phage to MAB383 and MAB664. Note that within the phage titers of 5×10^8 to 1.6×10^{10}, the KDR phage binds to all three antibodies in a dose-dependent, linear fashion, and the three binding curves closely overlap to each other.

scanning mutagenesis are generally consistent with this observation (Table II). Mutations in clusters 1 (M1) and 4 (M4) reduced the binding to MAB664 by ~50% and 93% but had no effect on binding to MAB383. In contrast, mutations in cluster 5 (M5) severely reduced binding to MAB383 while retaining reactivity to MAB664. Mutations in cluster 3 (M3) showed no effects on binding to either antibody. It is of interest that mutations in cluster 2 (M2) abolished binding to both MAB383 and MAB664. In contrast, mutations located to β-strand C′ (M6) abolished selectively the binding to MAB664. These results suggest that the multiple alanine mutations in cluster mutant M2 may have caused misfolding of the domain displayed on phage surface and/or local conformation disruption.

To identify the specific residues within the cluster mutants most critical for individual monoclonal antibody binding, a series of alanine-back-to-wild type mutants were constructed and tested (Table II). In the back mutants, the alanine mutations within the clustered mutants were changed individually back to the wild type residue. A single back mutation in M1, A238V (M1.1), fully restored the binding to MAB664, whereas another single back mutation in M4, A295D (M4.1), restored ~60% of the binding to MAB664. None of the single back mutations in M2 and M6 restored the binding to MAB664. As expected, none of the back mutations in M1 and M4 showed any effects on binding to MAB383.

Two individual back mutations in M5, A313L (M5.1) and A315T (M5.2), restored the binding to MAB383 by ~42% and 57%, respectively. Although none of the other three single back mutations in this region, A317K (M5.3), A319S (M5.4), or A326E (M5.5), restored the binding to MAB383, the combination of all three (M5.6) resulted in a mutant that demonstrated 43% binding activity of the wild type domain 3. In contrast to those seen with MAB664, single back mutations in M2, A256I (M2.1) and A261E (M2.3), each resulted in a mutant with 70–80% binding capacity to MAB383. A combined mutant (M2.8) with five back mutations (A261E, A262Y, A264S, A267H, and A268Q) bound as well as the wild type domain 3 to both MAB383 and MAB664. Converting the Glu^{261} in mutant M2.8 to alanine to create mutant M2.9, however, selectively reduced the binding to MAB383 by ~50%. As expected, none of the individual back mutations in M6 affected the binding to MAB383, nor did those in M5 have any effects on binding to MAB664 (Table II).

Construction and Expression of KDR (1–3) Variants in Mammalian Cells—We have identified key residues in KDR extracellular region most critical for binding to MAB383 and MAB664 using phage displayed domain 3 (Table II). It is not possible, however, to test the alanine mutants in this system for binding to VEGF and IMC-1C11, because both of them require domains 1–3 for efficient binding. To test whether the residues critical for MAB383 and MAB664 binding would also influence binding to VEGF and IMC-1C11, we introduced the alanine mutations into a KDR (1–3) construct and expressed the variant proteins in COS cells. In total, six KDR (1–3) variants (V1–V6) were prepared, with each variant containing exact the same cluster alanine mutations as in their respective phage-displayed domain 3 mutants (M1–M6; Tables II and III). The KDR (1–3) variant proteins were assayed in ELISA for binding to MAB383, MAB664, IMC-1C11, and VEGF. A diabody, DAB p3S5, which binds to KDR domain 1, was used in all ELISA to demonstrate the functional expression of the variant proteins and to normalize the amounts of protein added in the assay.

Consistent with our observations in the phage ELISA, the identical alanine mutations in cluster 3 (V3) did not have any effects on binding of KDR (1–3) to both MAB383 and MAB664 (Table III). Mutations in cluster 1 (V1) had no effect on binding MAB383, and caused ~20% reduction in binding to MAB664, which is less severe than that seen in phage-based ELISA (Tables II and III). Mutations in cluster 5 (V5) selectively abolished binding to MAB383 but had no effect on binding MAB664 (Table III). Two back mutations, A313L and A315T (V5.1), restored 73% of the binding of V5 to MAB383 (Table III). This confirmed our observation in phage-based ELISA, demonstrating that these two residues are important for MAB383 binding (Table II). Alanine mutations in cluster 4 in the context of KDR (1–3) (V4) did not, however, affect binding to MAB664. All above KDR (1–3) variants bind as well as wild type KDR (1–3) to IMC-1C11 and the natural ligand, VEGF (Table III), both of which require all the first three N-terminal domains for high affinity binding (Fig. 2).

The KDR (1–3) variant (V2) with multiple alanine mutations in cluster 2 failed to bind either MAB383 or MAB664 (Table III). This is consistent with our observation with the phage-displayed cluster mutant, M2 (Table II). Binding of V2 to VEGF and IMC-1C11 was only 10% to 20% of that of wild type KDR (1–3) protein. Our epitope mapping studies with KDR deletion mutants (Fig. 2), plus the phage-based ELISA (Table II), sug-

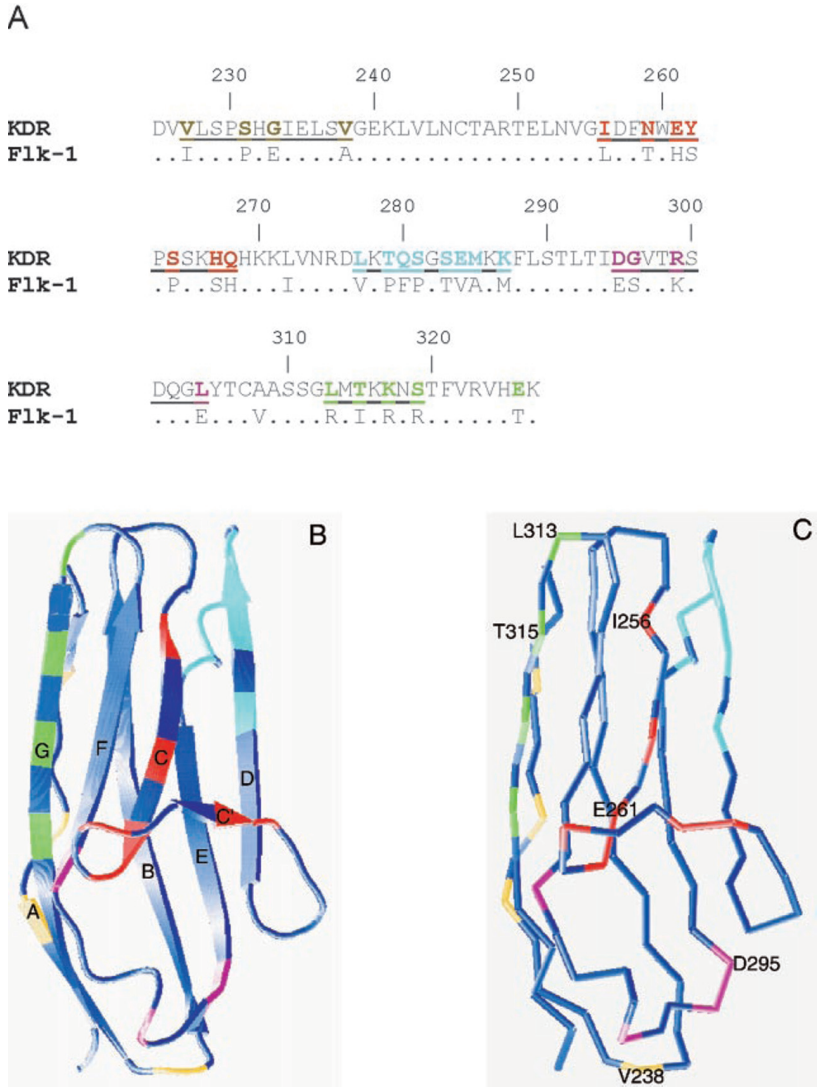

FIG. 4. *A*, amino acid alignment of the domain 3 from KDR and Flk-1. The residues within the cluster 1 mutant (M1) are shown in *yellow*, cluster 2 (M2) is in *red*, cluster 3 (M3) is in *blue*, cluster 4 (M4) is in *pink*, and cluster 5 (M5) is in *green*. *B*, model of KDR domain 3 with the β strands depicted as *arrows* and connecting residues as *tubes*. The cluster mutants are colored as in *A*, and the individual strands are lettered *A–G*. *C*, an α-carbon trace of KDR domain 3 with the same view as in *B*. Important residues identified by alanine mutagenesis with phage displayed KDR domain 3 are numbered.

gest that the neutralizing antibodies, MAB383, MAB664, and IMC-1C11, most likely bind to different epitopes within the KDR domain 3. Taken together, these results indicate a critical structure within this region of KDR for high affinity VEGF binding. Recently, Piossek *et al.* (28) demonstrated that a peptide from KDR domain 3 comprising residues ^{249}RTELNVGIDFNWEYP^{263} was capable of binding VEGF and inhibiting of VEGF-induced activation of KDR. A systematic replacement with L-amino acid within the peptide revealed the Asp^{257} as the hydrophilic key residue for VEGF binding (28). To further dissect out the critical residue(s) within cluster for binding to VEGF and to our anti-KDR monoclonal antibodies, we constructed and expressed six additional KDR (1–3) variants (V2.1-V2.6) (Table III).

A single alanine mutation within the cluster 2 region, I256A (V2.1), caused about 40% reduction in binding to MAB383. Another mutation, D257A, alone (V2.2) or in combination with I256A (V2.3), abolished binding to MAB383. The addition of a N253A mutation to V2.1 to create variant V2.4 had no effect on binding to MAB383. The binding was severely reduced, however, when Glu^{261} was mutated to alanine in the context of V2.4 (V2.5). Binding to IMC-1C11 of the above three KDR (1–3) variants was not affected, whereas binding to VEGF was reduced by ~30–40% as compared with that of wild type KDR (1–3) (Table III).

The binding pattern of KDR (1–3) variants to MAB664 is totally different from that to MAB383. None of the above mutations, I256A, D257A, and N253A, either alone or in various combinations, affected significantly binding to MAB664. Mutations in the C-terminal half of the cluster region, Y262A, S264A, H267A, and Q268A (V2.6), however, severely reduced the binding to MAB664 with no effect on binding to MAB383, IMC-1C11, and VEGF. Another cluster mutant in the region, Y262A, P263A, S264A, S265A, and K266A (V6) completely abolished the binding to MAB664. Binding to MAB383, IMC-1C11, and VEGF was also moderately affected by the clustered alanine mutations.

Combination of V2.5 (the variant with poor MAB383 binding) and V2.6 (the variant with poor MAB664 binding) resulted in a variant (V2) that failed to bind both MAB383 and MAB664. It is interesting to note that the binding of V2 to both IMC-1C11 and VEGF was also greatly reduced, although neither of the cluster mutations by itself (in V2.5 and V2.6) significantly affected the binding (Table III).

Molecular Modeling of KDR Domain 3—We built a model of KDR domain 3 to relate the mutagenesis data with structural information (Figs. 4 and 5). The mutagenesis results indicate that the domain 3 face made up from β-strands C, F, and G (Fig. 4*B*) is involved in binding the neutralizing anti-KDR antibodies and VEGF. The analogous face for domain 2 of Flt-1 was shown to be involved in binding VEGF (25).

In our model, the cluster 3 mutations (M3) are localized on

TABLE II
Binding of KDR mutant phage to antibodies MAB383 and MAB664

WT[a] Mutant	Amino acid sequence[b]	MAB383	MAB664
WT1	DVV^{227}LSPS^{231}HG^{233}IELSV^{238}GEK	1.0	1.0
M1	DV**A**^{227}LSP**A**^{231}H**A**^{233}IELS**A**^{238}GEK	0.91 ± 0.02[c]	0.51 ± 0.04
M1.1	DV**A**LSP**A**H**A**IELS**V**^{238}GEK	1.08 ± 0.10	**1.05 ± 0.02**
WT2	NVGI^{256}DFN^{259}WE^{261}Y^{262}PS^{264}SKH^{267}Q^{268}HKK	1.0	1.0
M2	NVG**A**^{256}DF**A**^{259}W**A**^{261}**A**^{262}P**A**^{264}SK**A**^{267}**A**^{268}HKK	0.07 ± 0.01	0.07 ± 0.03
M2.1	NVG**I**^{256}DF**A**W**AA**P**A**SK**AA**HKK	**0.70 ± 0.07**	0.07 ± 0.03
M2.2	NVG**A**DF**N**^{259}W**AA**P**A**SK**AA**HKK	0.11 ± 0.01	0.08 ± 0.01
M2.3	NVG**A**DF**A**W**E**^{261}**A**P**A**SK**AA**HKK	**0.81 ± 0.01**	0.06 ± 0.02
M2.4	NVG**A**DF**A**W**A**Y^{262}P**A**SK**AA**HKK	0.14 ± 0.04	0.04 ± 0.01
M2.5	NVG**A**DF**A**W**AA**PS^{264}SK**AA**HKK	0.07 ± 0.01	0.06 ± 0.02
M2.6	NVG**A**DF**A**W**AA**P**A**SKH^{267}**A**HKK	0.10 ± 0.01	0.09 ± 0.03
M2.7	NVG**A**DF**A**W**AA**P**A**SK**AQ**^{268}HKK	0.04 ± 0.01	0.05 ± 0.01
M2.8	NVG**A**DF**A**W**E**^{261}**Y**^{262}P**S**^{264}SK**H**^{267}**Q**^{268}HKK	**1.09 ± 0.06**	0.99 ± 0.05
M2.9	NVG**A**DF**NWA**Y^{262}P**S**^{264}SK**H**^{267}**Q**^{268}HKK	**0.56 ± 0.03**	0.72 ± 0.16
WT3	NRDL^{277}KT^{279}Q^{280}S^{281}GS^{283}E^{284}M^{285}KK^{287}FLS	1.0	1.0
M3	NRD**A**^{277}K**A**^{279}**A**^{280}**A**^{281}G**A**^{283}**A**^{284}**A**^{285}K**A**^{287}FLS	0.97 ± 0.07	0.98 ± 0.04
WT4	LTID^{295}G^{296}VTR^{299}SDQGL^{304}YTC	1.0	1.0
M4	LTI**A**^{295}**A**^{296}VT**A**^{299}SDQG**A**^{304}YTC	0.89 ± 0.03	0.22 ± 0.04
M4.1	LTI**D**^{295}**A**VT**A**SDQG**A**YTC	1.09 ± 0.01	**0.58 ± 0.05**
M4.2	LTI**AG**^{296}VT**A**SDQG**A**YTC	0.90 ± 0.10	0.08 ± 0.02
M4.3	LTI**AA**VT**R**^{299}SDQG**A**YTC	0.87 ± 0.09	0.21 ± 0.03
M4.4	LTI**AA**VT**A**SDQG**L**^{304}YTC	0.64 ± 0.02	0.23 ± 0.04
WT5	SSGL^{313}MT^{315}KK^{317}NS^{319}TFVRVHE^{326}KPF	1.0	1.0
M5	SSG**A**^{313}M**A**^{315}K**A**^{317}N**A**^{319}TFVRVH**A**^{326}KPF	0.21 ± 0.02	0.78 ± 0.10
M5.1	SSG**L**^{313}M**A**K**A**N**A**TFVRVH**A**KPF	**0.42 ± 0.08**	0.69 ± 0.06
M5.2	SSG**A**M**T**^{315}K**A**N**A**TFVRVH**A**KPF	**0.57 ± 0.07**	0.94 ± 0.22
M5.3	SSG**A**M**A**K**K**^{317}N**A**TFVRVH**A**KPF	0.21 ± 0.03	0.64 ± 0.09
M5.4	SSG**A**M**A**K**A**NS^{319}TFVRVH**A**KPF	0.34 ± 0.02	0.95 ± 0.12
M5.5	SSG**A**M**A**K**A**N**A**TFVRVH**E**^{326}KPF	0.25 ± 0.01	0.61 ± 0.05
M5.6	SSG**A**M**A**K**K**^{317}N**S**^{319}TFVRVH**E**^{326}KPF	**0.43 ± 0.09**	1.69 ± 0.19
WT6	NVGIDFNWE^{261}Y^{262}P^{263}S^{264}S^{265}K^{266}HQHKK	1.0	1.0
M6	NVGIDFNW**A**^{261}**A**^{262}**A**^{263}**A**^{264}**A**^{265}**A**^{266}HQHKK	0.64 ± 0.07	0.01 ± 0.0
M6.1	NVGIDFNW**E**^{261}**AAAAA**HQHKK	0.99 ± 0.01	0.02 ± 0.01
M6.2	NVGIDFNW**A**Y^{262}**AAAA**HQHKK	0.91 ± 0.16	0.02 ± 0.0
M6.3	NVGIDFNW**AA**P^{263}**AAA**HQHKK	0.74 ± 0.04	0.03 ± 0.01
M6.4	NVGIDFNW**AAA**S^{264}**AA**HQHKK	0.67 ± 0.06	0.01 ± 0.01
M6.5	NVGIDFNW**AAAA**S^{265}**A**HQHKK	0.88 ± 0.04	0.01 ± 0.0
M6.6	NVGIDFNW**AAAAA**K^{266}HQHKK	0.49 ± 0.01	0.01 ± 0.0

[a] The wild type (WT) sequences (WT1–WT6) are shown and numbered as in Fig. 4*A*. The residues targeted for alanine mutagenesis are marked by numbers on the upper right corner.

[b] Alanine mutations are shown in bold type and underline, whereas the back mutations are in bold type only. All alanine mutations in cluster mutants (M1, M2, M3, M4, M5, and M6) are also marked by numbers on the upper right corner. In back mutants (M1.1–M6.6), only the alanine-back-to-wild type mutations are marked by numbers.

[c] Numbers represent relative binding of each mutant to anti-KDR antibodies as compared to the wild type domain 3 (see "Experimental Procedures" for details). All data are the means ± S.E. of three–five separate experiments. The back mutants with at least 2-fold increase in binding compared with their respective cluster mutants are shown in bold type.

the opposite face, and the binding data support this; the M3 mutant has no effect on MAB383 or MAB664 binding. The model and binding data are consistent in localizing the MAB383 and MAB664 binding sites to discrete regions. The residues found to be significant for MAB664 binding are located in the "center" and "lower" half of the β-sheet face as depicted in Figs. 4*C* and 5*A*. In contrast, the important residues for MAB383 binding, Leu^{313}, Thr^{315}, Ile^{256}, and Glu^{261}, are situated on the "upper" half of the domain face (Figs. 4*C* and 5*A*).

The binding data implicate residues within β-strands C and C′ as central for binding to both VEGF and the neutralizing anti-KDR antibodies (for example mutants V2, V6, and V2.2). We hypothesize that this region of KDR, which in our model protrudes out from the surface (Fig. 5*B*), makes close contact with VEGF. Both overall shape complementarity and specific side chain interactions likely contribute to high affinity ligand binding.

DISCUSSION

Systematic domain deletion studies carried out with several tyrosine kinase receptors of the immunoglobulin superfamily, including Flt-1 (29–31), Kit-1 (32, 33), receptors for platelet-derived growth factor α (34), and fibroblast growth factor (35), have demonstrated that domains 1–3 are important for efficient ligand binding. Our results demonstrated that KDR domains 1–3 are necessary and sufficient for high affinity binding of VEGF (Fig. 2). Deletion of domain 3 completely abolished the binding of VEGF, indicating a critical role for this domain in KDR/VEGF interaction. This is in good agreement with those reported in the literature (16, 17). On the other hand, several studies have suggested that domains 2 and 3 constitute the minimal unit required for VEGF binding. For example, a dimeric KDR (2–3)-Fc fusion protein was shown to bind to VEGF with only 2-fold lower affinity than the intact KDR (1–7)-Fc fusion (16). Our results indicate that KDR domain 1 plays a role in high affinity binding to VEGF, because KDR (2–7) showed a much weaker binding to VEGF than KDR (1–7) (Fig. 2). This discrepancy is likely due to the choice of the domain boundaries plus the fusion partner for the deletion mutants. In the report of Fuh *et al*. (16), the KDR (2–3) construct consists of amino acids 1–335 (with 24–116 deleted) compared with our construct, KDR (2–7), where the entire N-terminal 1–123 amino acids were deleted. Further, Fuh *et al*. chose IgG Fc fragment as the fusion partner, which led to the production of bivalent KDR domain-Fc fusion proteins, in contrast to our monovalent KDR domain-AP fusion proteins. The affinities of bivalent KDR (1–7)-Fc and KDR (1–3)-Fc fusion proteins were

TABLE III
Binding of KDR(1–3) variants to neutralizing anti-KDR antibodies and VEGF

WT[a] Variant	Amino acid sequence[b]	MAB383	MAB664	IMC-1C11	VEGF
WT1	DVV^{227}LSPS^{231}HG^{233}IELSV^{238}GEK	1.0	1.0	1.0	1.0
V1	DV**A**^{227}LSP**A**^{231}H**A**^{233}IELS**A**^{238}GEK	0.95 ± 0.04[c]	0.80 ± 0.02	1.0	1.18 ± 0.03
WT2	NVGI^{256}D^{257}FN^{259}WE^{261}Y^{262}PS^{264}SKH^{267}Q^{268}HKK	1.0	1.0	1.0	1.0
V2	NVG**A**^{256}DF**A**^{259}W**A**^{261}**A**^{262}P**A**^{264}SK**A**^{267}**A**^{268}HKK	0.01 ± 0.01	0.01 ± 0.0	0.20 ± 0.01	0.09 ± 0.01
V2.1	NVG**A**^{256}DFNWEYPSSKHQHKK	0.58 ± 0.03	0.86 ± 0.01	0.93 ± 0.02	0.63 ± 0.06
V2.2	NVGI**A**^{257}FNWEYPSSKHQHKK	0.04 ± 0.01	0.74 ± 0.01	0.78 ± 0.01	0.68 ± 0.02
V2.3	NVG**A**^{256}**A**^{257}FNWEYPSSKHQHKK	0.05 ± 0.03	1.10 ± 0.06	1.16 ± 0.03	1.09 ± 0.07
V2.4	NVG**A**^{256}DF**A**^{259}WEYPSSKHQHKK	0.82 ± 0.01	1.07 ± 0.02	0.96 ± 0.05	0.61 ± 0.02
V2.5	NVG**A**^{256}DF**A**^{259}W**A**^{261}YPSSKHQHKK	0.11 ± 0.01	0.97 ± 0.02	0.85 ± 0.03	0.54 ± 0.01
V2.6	NVGIDF**A**^{259}WE**A**^{262}P**A**^{264}SK**A**^{267}**A**^{268}HKK	0.94 ± 0.21	0.02 ± 0.02	0.92 ± 0.22	0.92 ± 0.20
WT3	NRDL^{277}KT^{279}Q^{280}S^{281}GS^{283}E^{284}M^{285}KK^{287}FLS	1.0	1.0	1.0	1.0
V3	NRD**A**^{277}K**A**^{279}**A**^{280}**A**^{281}G**A**^{283}**A**^{284}**A**^{285}K**A**^{287}FLS	1.02 ± 0.02	1.33 ± 0.0	0.97 ± 0.01	0.9 ± 0.02
WT4	LTID^{295}G^{296}VTR^{299}SDQGL^{304}YTC	1.0	1.0	1.0	1.0
V4	LTI**A**^{295}**A**^{296}VT**A**^{299}SDQG**A**^{304}YTC	0.88 ± 0.01	1.10 ± 0.02	0.97 ± 0.01	1.03 ± 0.01
WT5	SSGL^{313}MT^{315}KK^{317}NS^{319}TFVRVHE^{326}KPF	1.0	1.0	1.0	1.0
V5	SSG**A**^{313}M**A**^{315}K**A**^{317}N**A**^{319}TFVRVH**A**^{326}KPF	0.01 ± 0.0	0.68 ± 0.02	0.73 ± 0.01	0.69 ± 0.01
V5.1	SSGLMTK**A**^{317}N**A**^{319}TFVRVH**A**^{326}KPF	0.73 ± 0.12	0.71 ± 0.01	1.03 ± 0.14	0.89 ± 0.12
WT6	NVGIDFNWE^{261}Y^{262}P^{263}S^{264}S^{265}K^{266}HQHKK	1.0	1.0	1.0	1.0
V6	NVGIDFNWE**A**^{261}**A**^{262}**A**^{263}**A**^{264}**A**^{265}HQHKK	0.49 ± 0.01	0.01 ± 0.01	0.51 ± 0.02	0.42 ± 0.01

[a] The wild type (WT) sequences (WT1–WT6) are shown and numbered as in Fig. 4*A*. The residues targeted for alanine mutagenesis are marked by numbers on the upper right corner.

[b] Alanine mutations are shown in bold type and marked by numbers on the upper right corner. Cluster variants (V1, V2, V3, V4, V5, and V6) contain exactly the same cluster alanine mutations, in KDR(1–3) context, as in their respective phage-displayed domain 3 mutants (M1, M2, M3, M4, M5, and M6) described in Table II.

[c] Numbers represent relative binding of each variant to anti-KDR antibodies or VEGF as compared to the wild type KDR(1-3) (see "Experimental Procedures" for details). All data are the means ± S.E. of three–five separate experiments.

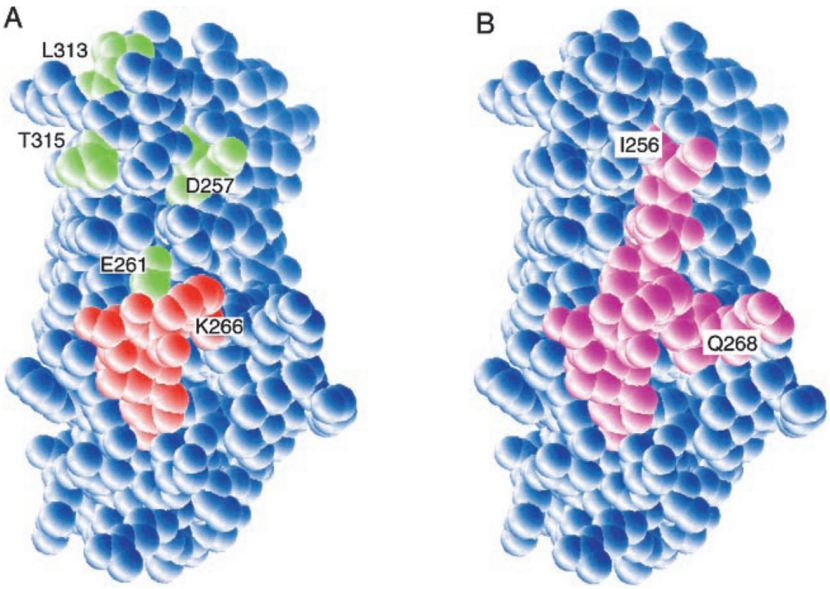

FIG. 5. *A*, space-filling model of KDR domain 3. The residues important for MAB383 binding are in *green*, and the important residues for MAB664 binding are in *red*. *B*, the residues determined to be central for VEGF binding are in *pink* in this space-filling model of KDR domain 3.

shown to be ~100- and 33-fold higher than those of their monovalent counterparts, respectively (16). The exact role of domain 1 in KDR/VEGF interaction, however, has not been well defined to date. KDR mutant-Fc fusion proteins lacking the domain 1 showed a slightly higher association rate to VEGF compared with those fusion proteins having this domain, indicating that domain 1 may negatively regulate the ligand binding by partially shielding the VEGF recognition domains of the receptor (36). A similar function is also proposed for domain 1 in Flt-1; it may shield the hydrophobic surface of domain 2 in the absence of ligand but is displaced by the ligand upon receptor-ligand complex formation (25).

Because KDR domain 3 is most critical for KDR/VEGF interaction, it is not surprising that all three neutralizing anti-KDR antibodies we tested here, MAB383, MAB664, and IMC-1C11, required the presence of domain 3 for efficient binding. Although IMC-1C11 demonstrated a binding pattern similar to the natural ligand, VEGF, both MAB383 and MAB664 require only domain 3 for binding. It is interesting to note that several non-neutralizing anti-KDR antibodies developed in our laboratory, including MAB413 (18), DAB p3S5 (21), scFv p2A6 (19), and scFv p4G7 (21), bind epitopes that are located either within KDR domain 1 (scFv p2A6 and DAB p3S5) or domain 6 and 7 (scFv p4G7 and MAB413). Further, MAKD6, a neutralizing anti-KDR antibody, was shown to bind to an epitope within KDR domain 2 (16). Taken together, these results suggest that KDR/VEGF interaction may occur across the receptor interface that is composed mainly of KDR domains 2 and 3. The neutralizing anti-KDR antibodies are likely to exert their activity by either directly competing with VEGF for binding or by causing steric hindrance once bound to the receptor.

Alanine-scanning mutagenesis was used to dissect the binding epitopes on KDR domain 3 for neutralizing antibodies. In our preliminary study, we tried to display KDR domains 1–3 on the phage surface. The resulting phage particles, although reactive to anti-E tag antibody, failed to bind any of the anti-

KDR antibodies. We believe the failure is likely due to incorrect folding and/or the lack of glycosylation of the KDR domains displayed on the surface of M13 bacteriophage. On the other hand, phage particles displaying the single domain 3 binds efficiently to both MAB383 and MAB664 (Fig. 3), suggesting that the domain is properly folded and functionally displayed on the surface. Phage treated with factor Xa or reducing agent, dithiothreitol, showed greatly reduced binding to both antibodies, further confirming that the phage/antibody interaction is a specific event.

In general, high affinity protein-protein interactions are dependent on both the direct contact residue(s) and on shape complementarity of the binding surfaces. Alteration of the contact residues or disruption of the structural conformation of KDR may lead to the loss of antibody and/or VEGF binding. Without crystal structural information of KDR, we cannot rule out the possibility that some of the alanine mutations influence antibody and/or VEGF binding by disturbing domain folding or altering β sheet conformation within the receptor. Utilizing several anti-KDR antibodies that recognize different epitopes on the receptor help distinguish between these possibilities. We believe the majority of our alanine mutants, perhaps with only the exception of mutant M2 (Table II) and variant V2 (Table III), maintain their overall structure because they retained their binding to at least two of four anti-KDR antibodies and/or the ligand, VEGF (Tables II and III).

Our studies locate the binding epitopes in cluster 2 (Ile^{256}, Asp^{257}, and Glu^{261} in β-strand C) and cluster 5 (Leu^{313} and Thr^{315} in β-strand F) for MAB383 (Table III). Two single mutations, D257A (V2.2) and E261A (V2.5), each abolished the antibody binding. Both Asp^{257} and Glu^{261} are negatively charged and exposed on the surface and thus are available for direct contact with MAB383 (Fig. 5*A*). In contrast, the Ile^{256} side chain is buried, packing in the interior of the domain, and likely affects antibody binding indirectly by influencing the conformation of the contact residue, Asp^{257}. Mutations of Leu^{313} and Thr^{315} resulted in a mutant (M5.6) with reduced binding to MAB383. The Thr^{315} side chain is directed out from β-strand G and may make direct contact with the antibody (Fig. 5*A*). On the other hand, the Leu^{313} side chain is only partly exposed and may contribute to surface complementarity. It is noteworthy that although MAB383 competes with IMC-1C11 for binding to KDR (Table I), the alanine mutations that interfere with MAB383 binding did not have any significant effects on binding to IMC-1C11 (Table III). The competition between MAB383 and IMC-1C11, therefore, may be due to steric hindrance. Alternately, there may be other residues within domain 3 that MAB383 and IMC-1C11 share that we have not identified.

The residues important for MAB664 binding, Tyr^{262}, Pro^{263}, Ser^{264}, Ser^{265}, Lys^{266}, His^{267}, and Gln^{268}, are distinct from those for MAB383. These residues are located in β-strands C, C′, and the turn that connects them (Fig. 4*B*), a region that forms a protrusion on the surface of the protein. The side chains of these residues are predicted to play a role in both maintaining the structural integrity of the protrusion and in making direct contact with MAB664. Alanine mutations at Tyr^{262}, Pro^{263}, His^{267}, and Gln^{268} (V2.6) did not cause any global structural changes since the variant retained full reactivity to MAB383, IMC-1C11 and VEGF. The binding to MAB664, however, was totally abolished by these mutations. Variant (V6) with alanine mutations at Tyr^{262}, Pro^{263}, Ser^{264}, Ser^{265}, and Lys^{266} also lost its binding to MAB664. The latter alanine mutations, however, may have caused some local conformation change since the binding of the variant V6 to the other two antibodies as well as to VEGF was also reduced by ~50% (Table III). In contrast to phage-based analysis, alanine mutations in cluster 4 in the context of KDR (1–3) did not show any detrimental effect on binding to MAB664 (Table III). The discrepancy may be due to the difference in the context in which the assays were performed. The effects of mutations in domain 3 in the KDR (1–3) context could be, more or less, compensated by the presence of the other two domains. No overlapping residues were seen between the binding epitopes of MAB383 and MAB664. This is consistent with our previous observation that MAB383 and MAB664 do not compete with each other for receptor binding (Table I). Finally, alanine mutations in cluster 3 (β-strand D and E) did not show any effects on binding to VEGF and to all three anti-KDR antibodies in both phage and KDR (1–3)-based ELISA (Table II and III). This result is in good agreement with our model showing that all the alanine mutations within this region are located on the back face of the molecule, *i.e.* they are point away from the binding surface for VEGF and neutralizing anti-KDR antibodies (Fig. 4*B*).

As expected, combination of V2.5 (the variant with poor MAB383 binding) and V2.6 (the variant with poor MAB664 binding) resulted in a variant (V2) that failed to bind both MAB383 and MAB664. The binding of V2 to IMC-1C11 and VEGF was also greatly reduced, although both V2.5 and V2.6 bind well to IMC-1C11 and VEGF. These results suggest that multiple alanine mutations in this region most likely have caused dramatic structure changes within domain 3 (Fig. 5*B*). Recently, Piossek *et al.* (28) demonstrated that residue Asp^{257} as the key hydrophilic residue for VEGF binding. In our study, the single D257A mutation (V2.2) in the context of KDR (1–3) only mildly decreased VEGF binding. The binding of variant V2.2 to the two other antibodies, MAB664 and IMC-1C11, was also moderately affected (Table III). In contrast, the single alanine mutation completely abolished the binding of MAB383, strongly indicating Asp^{257} as a contact residue for the antibody.

Unlike MAB383 and MAB664, IMC-1C11 and VEGF require domains 1–3 of KDR for efficient binding (Fig. 1). We note that IMC-1C11 and VEGF follow the same binding pattern to various KDR deletion mutants (Fig. 2) and alanine variants (Table III). In fact, IMC-1C11 was the only neutralizing antibody (out of more than a dozen tested) that mimics VEGF in binding to the receptor (18–21). IMC-1C11 was derived from a scFv originally isolated from a phage display library constructed from the splenocytes of a mouse immunized with soluble KDR protein (19, 20). Our previously studies have demonstrated that IMC-1C11 competed effectively with VEGF for binding to KDR and blocked VEGF-induced receptor activation and mitogenesis of human endothelial cells (20). In addition, IMC-1C11 inhibited pathological angiogenesis in oxygen-induced proliferative retinopathy in a new born dog model.[3] Taken together, these results lend strong support to clinical evaluation of IMC-1C11 as anti-angiogenesis agent.

In conclusion, we have mapped the binding epitopes within KDR domain 3 for neutralizing anti-KDR antibodies, MAB383 and MAB664, using a structural alignment plus alanine-scanning mutagenesis. A subset of residues critical for binding to neutralizing anti-KDR antibodies was also found to be important for VEGF binding. Further, IMC-1C11 was identified to possess the same receptor-binding properties as the natural ligand, VEGF. It is likely that other residues within KDR domain 3 or other domains also play roles in antibody and VEGF binding and/or in maintaining the structural integrity of the receptor because only a selected group of residues were

[3] D. S. McLeod, M. Taomoto, J. Cao, Z. Zhu, L. Witte, and G. A. Lutty, *et al.,* submitted for publication.

targeted for alanine mutagenesis in this study. Definitive answers will only be provided by the crystal structure of complexes between KDR/VEGF and KDR/antibody.

REFERENCES

1. Terman, B. I., and Dougher-Vermazen, M. (1996) *Cancer Met. Rev.* **15,** 159–163
2. Millauer, B., Wizigmann-Voos, S., Schnurch, H., Martinez, R., Moller, N. P. H., Risau, W., and Ullrich, A. (1993) *Cell* **72,** 835–846
3. Quinn, T. P., Peters, K. G., De Vries, C., Ferrara, N., and Williams, L. T. (1993) *Proc. Natl. Acad. Sci. U. S. A.* **90,** 7533–7537
4. Ferrara, N. (1995) *Breast Cancer Res. Treat.* **36,** 127–137
5. Brown, L. F., Claffey, D. K., Nagy, J. A., Feng, D., Dvorak, A. M., and Dvorak, H. F. (1997) in *Regulation of Angiogenesis* (Goldberg, I. D., and Rosen, E. M. eds) pp. 233–269, Birkhauser Verlag, Basel, Switzerland
6. Zhu, Z., and Witte, L. (1999) *Invest. New Drugs* **17,** 195–212
7. Millauer, B., Shawver, L. K., Plate, K. H., Risau, W., and Ullrich, A. (1994) *Nature* **367,** 576–579
8. Kim, J., Li, B., Winer, J., Armanini, M., Gillett, N., Phillip, H. S., and Ferrara, N. (1993) *Nature* **362,** 841–844
9. Skobe, M., Rockwell, P., Goldstein, N., Vosseler, S., and Fusening, N. E. (1997) *Nat. Med.* **3,** 1222–1227
10. Pierce, E. A., Avery, R. L., Foley, E. D., Aiello, L. P., and Smith, L. E. H. (1995) *Proc. Natl. Acad. Sci. U. S. A.* **92,** 905–909
11. Koch, A. E., Harlow, L. A., Haines, G. K., Amento, E. P., Unemori, E. N., Wong, W. L., Pope, R. M., and Ferrara, N. (1994) *J. Immunol.* **152,** 4149–4156
12. Sun, P. D., and Davies, D. R. (1995) *Annu. Rev. Biophys. Biomol. Struct.* **24,** 269–291
13. Keyt, B. A., Nguyen, H. V., Berleau, L. T., Duarte, C. M., Park, J., Chen, H., and Ferrara, N. (1996) *J. Biol. Chem.* **271,** 5638–5646
14. Muller, Y. A., Li, B., Christinger, H. W., Wells, J., Cunningham, B., and de Vos, A. M. (1997) *Proc. Natl. Acad. Sci. U. S. A.* **94,** 7192–7197
15. Muller, Y. A., Christinger, H. W., Keyt, B. A., and de Vos, A. M. (1997) *Structure* **5,** 1325–1338
16. Fuh, G., Li, B., Crowley, C., Cunningham, B., and Wells, J. (1998) *J. Biol. Chem.* **273,** 11197–11204
17. Kaplan, J. B., Sridharan, L., Zaccardi, J. A., Dougher-Vermazen, M., and Terman, B. I. (1997) *Growth Factors* **14,** 243–256
18. Witte, L., Hicklin, D. J., Zhu, Z., Pytowski, B., Kotanides, H., Rockwell, P., and Bohlen, P. (1998) *Cancer Met. Rev.* **17,** 155–161
19. Zhu, Z., Rockwell, P., Lu, D., Kotanides, H., Pytowski, B., Hicklin, D. J., Bohlen, P., and Witte, L. (1998) *Cancer Res.* **58,** 3209–3214
20. Zhu, Z., Lu, D., Kotanides, H., Santiago, A., Jimenez, X., Simcox, T., Hicklin, D. J., Bohlen, P., and Witte, L. (1999) *Cancer Lett.* **136,** 203–213
21. Lu, D., Kotanides, H., Zhou, Q., Jimenez, X., Persuad, K., Bohlen, P., and Witte, L., and Zhu, Z. (1999) *J. Immunol. Methods* **230,** 159–171
22. Flanagan, J. G., and Leder, P. (1990) *Cell* **53,** 185–194
23. Cabilly, S., Heldman, J., Heldman, E., and Katchalski-Katzir, E. (1998) in *Combinatorial Peptide Library Protocol* (Cabilly, S., ed) pp. 175–183, Humana Press, Totowa, NJ
24. Holden, H. M., Ito, M., Hartshorne, D. J., and Rayment, I. (1992) *J. Mol. Biol.* **227,** 840–851
25. Wiesmann, C., Fuh, G., Christinger, H. W., Eigenbrot, C., Wells, J., and de Vos, A. M. (1997) *Cell* **91,** 695–704
26. Jones, T. A., Zou, J. Y., and Cowan, S. W. (1991) *Acta Crystallogr. A.* **47,** 110–119
27. Harpaz, Y., and Chothia, C. (1994) *J. Mol. Biol.* **238,** 528–539
28. Piossek, C., Schneider-Mergener, J., Schirner, M., Vakalopoulou, E., Germeroth, L., and Thierauch, K.-H. (1999) *J. Biol. Chem.* **274,** 5612–5619
29. Davis-Smith, T., Chen, H., Park, J., Presta, L. G., and Ferrara, N. (1996) *EMBO J.* **15,** 4919–4927
30. Cunningham, S. A., Stephan, C. C., Arrate, M. P., Ayer, K. G., and Brock, T. A. (1997) *Biochem. Biophys. Res. Commun.* **231,** 596–599
31. Barleon, B., Totzke, F., Herzog, C., Blanke, S., Kremmer, E., Siemeister, G., Marme, D., and Martiny-Baron, G. (1997) *J. Biol. Chem.* **272,** 10382–10388
32. Blechman, J. M., Lev, S., Barg, J., Eisenstein, M., Vaks, B., Vogel, Z., Givol, D., and Yarden, Y. (1995) *Cell* **80,** 103–113
33. Lemmon, M. A., Pinchasi, D., Zhou, M., Lax, I., and Schlessinger, J. (1997) *J. Biol. Chem.* **272,** 6311–6317
34. Mahadevan, D., Yu, J.-C., Saldanha, J. W., Thanki, N., McPhie, P., Uren, A., LaRochelle, W. J., and Heidaran, M. A. (1995) *J. Biol. Chem.* **270,** 27595–27600
35. Wang, F., Kan, M., Xu, J., Yan, G., and McKeehan, W. L. (1995) *EMBO J.* **270,** 10222–10230
36. Shinkai, A., Ito, M., Anazawa, H., Yamaguchi, S., Shitara, K., and Shibuya, M. (1998) *J. Biol. Chem.* **273,** 31283–31288